Am J Transl Res 2022;14(11):8380-8389
www.ajtr.org /ISSN:1943-8141/AJTR0146268

Original Article

MASM inhibits cancer stem cell-like characteristics of EpCAM$^+$ cells via AKT/GSK3β/β-catenin signaling

Keyan Sun*, Huaxing Shen*, Shipeng He, Ying Liu

*Institute of Translational Medicine, Shanghai University, No. 99 Shangda Road, Shanghai 200444, China. *Equal contributors.*

Received September 1, 2022; Accepted November 13, 2022; Epub November 15, 2022; Published November 30, 2022

Abstract: Objectives: Liver cancer stem cells (LCSCs) are regarded as the frequent cause of hepatocellular carcinoma (HCC) relapse and therapeutic resistance. The epithelial cell adhesion molecule (EpCAM) is one of the key biomarkers for LCSCs. EpCAM$^+$ cells from HCC have been reported to display cancer stem cell-like (CSC-like) properties. Therefore, we aimed to verify the effect of MASM, a novel derivative of matrine, on CSC-like properties of EpCAM$^+$ HCC cells. Methods: EpCAM$^+$ cells were isolated from Hep3B and Huh7 cells using the magnetic-activated cell sorting. The capacity for self-renewal and proliferation of EpCAM$^+$ HCC cells was determined by the sphere-formation and cell counting kit 8 assays. After these cell populations were exposed to increasing concentrations of MASM, sphere formation, cell proliferation, apoptosis, resistance to chemotherapy and colony formation were evaluated, respectively. Moreover, the stemness-associated gene expression and underlying mechanisms were evaluated by quantitative real-time polymerase chain reaction and sphere-forming assay. Results: MASM significantly inhibited proliferation without inducing apoptosis, down-regulated the expression of stemness-related genes, decreased the percentage of EpCAM$^+$ HCC cells and up-regulated mature hepatocyte-related genes. Moreover, MASM suppressed the formation and reduced the size of not only primary spheroids but also subsequent spheroids. Additionally, our results showed that MASM inhibited the AKT/GSK3β/β-catenin signaling pathway. Conclusion: MASM treatment is effective against EpCAM$^+$ cells and may be considered as a novel drug candidate in HCC therapy.

Keywords: Matrine derivative, hepatocellular carcinoma, cancer stem cells, AKT/GSK3β/β-catenin signaling

Introduction

Hepatocellular carcinoma (HCC) is the third most prevalent type of cancer worldwide. Despite the use of aggressive surgical resection and chemotherapy, the overall five-year mortality of advanced HCC patients with recurrent tumors still remains unsatisfactory [1-5]. Hence, it is imperative to establish unique treatment approaches for HCC.

Cancer stem cells (CSCs) play an important role in the recurrence and metastasis of HCC [6-9]. The epithelial cell adhesion molecule (EpCAM) has been used as a CSC marker in HCC [10, 11]. High expression of EpCAM in HCC cells were significantly correlated with a poor prognosis [12, 13]. Moreover, EpCAM$^+$ HCC cells exhibited CSC-like properties such as self-renewal, differentiation, tumorigenesis and chemoresistance [14-16]. Thus, liver cancer cells expressing CSC marker EpCAM might be recognized as a therapeutic target for HCC [17].

Matrine, a primary active alkaloid of the Chinese herbaceous drug *Sophora flavescens Ait*, has anti-inflammation, antivirus and anti-cancer features [18-22]. However, the potency of sophora alkaloids is restricted owing to their reasonably reduced actions and limited half-lives [23]. To enhance their curative impacts, we have semi-manufactured a number of secondary matrines by transforming the carbonyl oxygen atom with a sulfur atom and inserting different amino groups to the keto-beta location. MASM ((6aS, 10S, 11aR, 11bR, 11cS)-10-methylamino-dodecahydro-3a,7a-diazabenzo (de) anthracene-8-thione; **Figure 1A**) is one of the unique matrine derivatives with developed pharmacological actions compared with matrine and sophocarpine [24]. We have previously shown that MASM suppressed HCC cells, sphere cells and HCC xenograft growth via decreasing the AKT/GSK3β/β-catenin signaling pathway. In this study, we examined MASM for its effect on EpCAM$^+$ HCC cells, as well as the associated mechanisms.

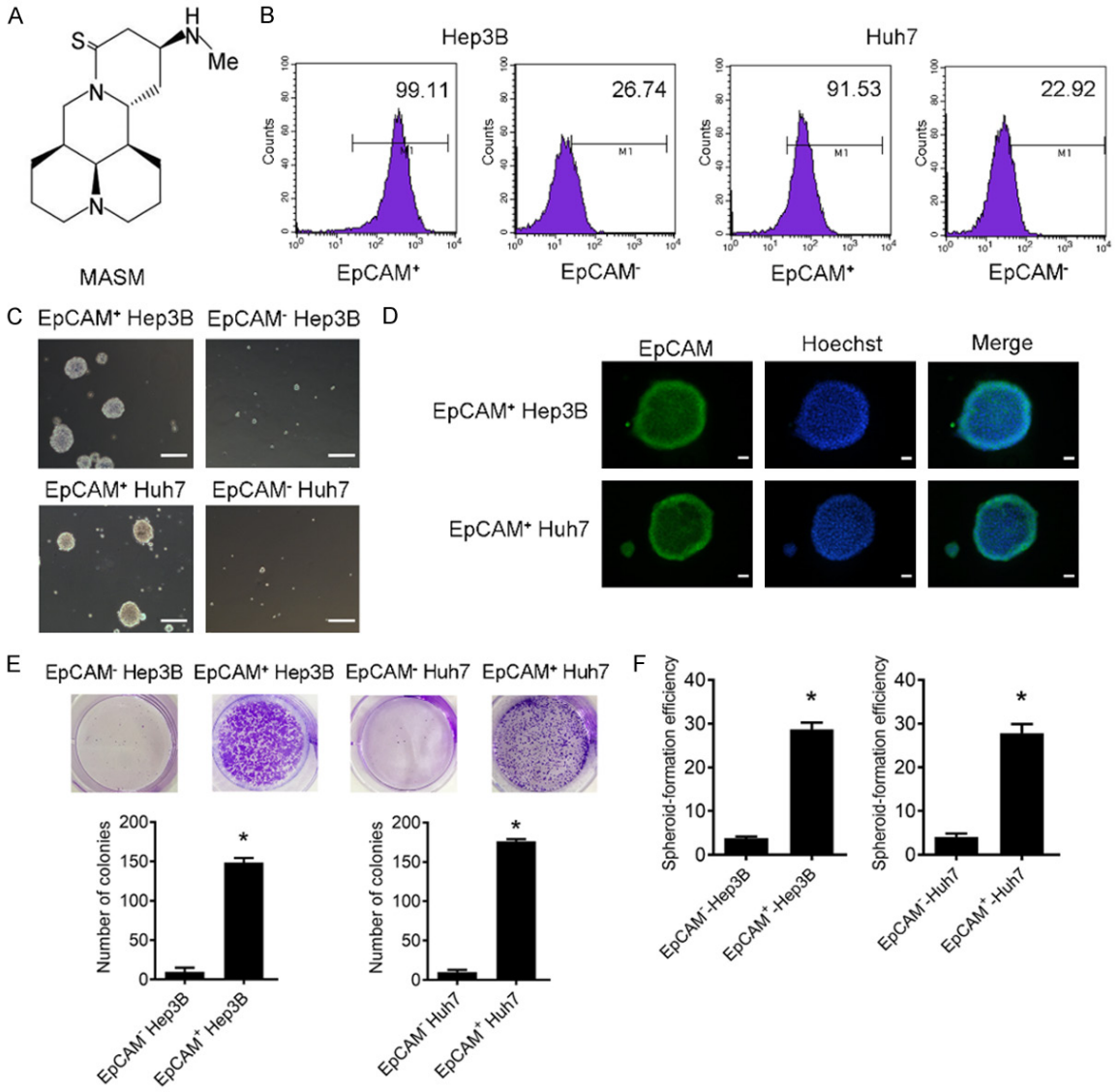

Figure 1. EpCAM+ Hep3B and Huh7 cells exhibit CSC-like properties. A. Chemical structure of MASM. B. Purity of the sorted EpCAM+ and EpCAM- cells from Hep3B and Huh7 was analyzed by flow cytometry. C. Representative image of spheres formed by EpCAM+ and EpCAM- cells isolated from Hep3B and Huh7 (scale bar = 200 μm). D. Isolated EpCAM+ and EpCAM- cells were immunostained with antibodies against EpCAM and counterstained with hoechst. Fluorescence images were captured with fluorescence microscope. Hoechst dye (blue) is for nuclear acid (nuclear) staining. Scale bar = 50 μm. E. Representative images of the plates including colonies obtained from EpCAM+ and EpCAM- cells. Colony experiments were performed in triplicate (mean ± SD). *$P < 0.05$ vs. EpCAM- cells. F. Sphere-forming efficiency of isolated EpCAM+ and EpCAM- cells cultured in serum-free conditions for 3-4 weeks, and spheres with diameter > 50 μm were counted. *$P < 0.05$ vs. EpCAM- cells.

Materials and methods

Cell lines and reagents

The human HCC cell lines Hep3B and Huh7 were generously donated by the Department of Gastroenterology, Shanghai Changzheng Hospital, Naval Medical University. In a 37°C medium with 5% CO_2, the cells were maintained in Dulbecco's modified Eagle's medium (DMEM) supplemented with 10% fetal bovine serum (ThermoFisher Scientific, MA, USA), 1% penicillin and streptomycin (Beyotime, Shanghai, China).

Michael addition was employed to create MASM maleate (> 98% purity), and the procedures were as described in a previous report

[24]. AKT inhibitor MK2206 and GSK3β inhibitor CHIR99021 were purchased from Selleck Chemicals (Shanghai, China).

Isolation of EpCAM+ and EpCAM- HCC cells

EpCAM antibodies combined with magnetic beads (Miltenyi Biotec, North Rhine-Westphalia, Germany) were mixed with individual cells. A magnetic column (Miltenyi Biotec, North Rhine-Westphalia, Germany) was employed to isolate the EpCAM+ cells. Flow cytometry was employed to examine the isolated cells.

Spheroids formation assay

After cell isolating, EpCAM+ cells were placed in 24-well ultralow dishes (Corning, NY, USA) and cultivated in DMEM/F-12 supplemented with recombinant human basic fibroblast growth factor, recombinant human epidermal growth factor, B27 (1 ×), ITS (1 ×) and L-glutamine (1 ×; Invitrogen, CA, USA). Sphere cells were trypsinized and resuspended at 1×10^3 cells in ultralow adherent 96-well plates (Corning, NY, USA), then subjected to different doses of MASM for one week. The second and third passages of the cells were cultured for 7 days without MASM. Under a phase contrast microscope, spheroids with diameters more than 50 μm were identified and captured on camera (Olympus, Tokyo, Japan).

Cell proliferation and colony formation assay

Isolated cells were placed in 96-well plates and exposed for 3 days to MASM at various doses (0-40 μmol/L). A cell counting kit 8 (CCK-8, Beyotime, Shanghai, China) was employed to measure cell proliferation. EpCAM+ or EpCAM- were cultured at 1×10^3 cells per well in 6-well plates for the colony formation experiment, and the cells were cultivated for 17 days to three weeks. Every three days, the culture media was replaced. Crystal violet (Beyotime, Shanghai, China) was employed to dye the colonies before being imaged.

Anti-EpCAM-PE antibody was kept with the cells in PBS including 1% bovine serum albumin. Isotype-matched mouse anti-IgG1-PE (Miltenyi Biotec, North Rhine-Westphalia, Germany) was used for controls. Samples were analyzed with a FACSCalibur flow cytometer (BD Biosciences, San Jose, CA, USA).

Immunofluorescence

Cells were stained with rabbit anti-EpCAM as primary antibody. FITC-conjugated anti-rabbit IgG was used as secondary antibody (Miltenyi Biotec, North Rhine-Westphalia, Germany). Then, cells were counterstained with Hoechst 33358 (Beyotime, Shanghai, China) and photographed under a phase contrast microscope (Olympus, Tokyo, Japan).

Apoptosis

The treated cells were resuspended in 0.5 mL (1×10^6 cells/mL) PBS, rinsed once more, and colored using the Annexin V-FITC and propidium iodide (PI) double-labeled flow cytometry kit (KeyGen, Nanjing, China). Cells were examined by a FACSCalibur flow cytometer.

Ammonia metabolism

Isolated cells were placed in 24-well plates and subjected to MASM for one week. Using the Ammonium Assay Kit (Hayward, CA, USA), ammonia concentration of the media was measured at 340 nm by using a microplate reader (BioTek Instruments, GA, USA).

Quantitative real-time polymerase chain reaction (qRT-PCR)

EpCAM+ cells were treated with MASM for the indicated times. Total RNA was extracted using the RNAfast200 kit (Fastagen Biotech Company, Shanghai, China). Then, 1 μg of RNA was transformed in cDNA using the PrimeScript RT reagent Kit (Takara, Dalian, China), and the PCR amplification was performed in triplicate on a StepOnePlusTM realtime PCR system (Applied Biosystems, USA) using the SYBR Premix Ex TaqTM PCR Kit (Takara, Dalian, China). The primer sequences for the genes are listed in **Table 1**.

Statistical analysis

All data were represented as the mean ± standard deviation (SD) and obtained from at least three independent experiments. Student's *t*-tests were used to assess statistical differences between two groups. The significance of differences among multiple groups was analyzed using two-way analysis of variance followed by Bonferroni's *post hoc* test via

Table 1. Sequence of primers

Gene	Sequence
β-actin	F: 5'-ACCCACACTGTGCCCATCTATG-3'
	R: 5'-AGAGTACTTGCGCTCAGGAGGA-3'
EpCAM	F: 5'-GCTCTGAGCGAGTGAGAACCT-3'
	R: 5'-GACCAGGATCCAGATCCAGTTG-3'
CD133	F: 5'-ACATGAAAAGACCTGGGGG-3'
	R: 5'-GATCTGGTGTCCCAGCATG-3'
Oct3/4	F: 5'-CGACCATCTGCCGCTTTGAG-3'
	R: 5'-CCCCCTGTCCCCCATTCCTA-3'
CK18	F: 5'-TCAACTTCCTCAGGCAGCTATATG-3'
	R: 5'-TGCTTCTGCTGGCTTAATG-3'
CK19	F: 5'-CGAAGCCAATATGAGGTC-3'
	R: 5'-CGGTTCAATTCTTCAGTCC-3'
CK8	F: 5'-TCAACTTCCTCAGGCAGCTATATG-3'
	R: 5'-GGTTGGCAATATCCTCGTACTGT-3'
AFP	F: 5'-TACGTCCCTCCACCATTTC-3'
	R: 5'-ATCCTGGTCTTTGCAGCACT-3'
ALB	F: 5'-AGCCTAAGGCAGCTTGACTT-3'
	R: 5'-CTCGATGAACTTCGGGATGA-3'

GraphPad Prism 8.0.1 software (GraphPad Software, La Jolla, CA, USA). $P < 0.05$ was considered as the minimum level of significance.

Results

Isolation and characterization of EpCAM+ cells in HCC

EpCAM+ and EpCAM- subpopulations were separated from Hep3B and Huh7 cells using magnetic-activated cell sorting, and a purity of 99.11% was found in sorted EpCAM+ Hep3B cells, and 91.53% in EpCAM+ Huh7 cells (**Figure 1B**). In a serum-free environment, the EpCAM+ population proliferated as floating spheroids, whereas most of the EpCAM- population died (**Figure 1C**). Spheroids obtained from EpCAM+ fraction were positive for EpCAM (**Figure 1D**). The colony formation assay showed that EpCAM+ cells from Hep3B and Huh7 cells were able to induce more and bigger colonies than EpCAM- cells (**Figure 1E**). Furthermore, EpCAM+ cells displayed higher spheroid-forming efficiency in spheroid-forming assays in comparison with the EpCAM- cells (**Figure 1F**).

CSCs have been reported to be more resistant to chemotherapy than other tumor cells [25]. We tested whether EpCAM+ and EpCAM- cells have different sensitivity to the therapeutic agents, doxorubicin (DOX) and 5-fluorouracil (5-FU). Isolated EpCAM+ and EpCAM- cells were subjected to different concentrations of DOX (0, 1, 2, and 5 μM) and 5-FU (0, 50, 100, and 200 μM) for 72 hours, and our data demonstrated that EpCAM+ cells were more resistant to DOX and 5-FU than EpCAM- cells (**Figure 2A**, **2B**).

Impacts of MASM on cell proliferation and apoptosis in EpCAM+ and EpCAM- cells

We compared the impact of MASM on the viability of isolated EpCAM+ and EpCAM- cells. The results revealed that MASM preferentially inhibited the EpCAM+ cells as compared with the EpCAM- cells (**Figure 3A**). To determine whether the inhibition of cell viability was through the induction of apoptosis in sorted cells, EpCAM+ and EpCAM- cells were detected with Annexin V-FITC and PI double staining. The results showed that MASM induced apoptosis of the EpCAM- cells in a dose-dependent manner, while it had a mild effect on the EpCAM+ cells (**Figure 3B**).

Effects of MASM on CSC-like properties of EpCAM+ HCC cells

We performed sphere formation assays to investigate the effect of MASM on the self-renewing capacity of EpCAM+ HCC cells. The results showed that MASM decreased the numbers and dimensions of primary spheroids (**Figure 4A**, **4B**). Furthermore, the number of spherical colonies significantly decreased when MASM-treated primary spheroids were cultured for the subsequent two passages in the absence of drug (**Figure 4C**). In EpCAM+ cells, MASM reduced the expression of stem cell biomarkers and raised the expression of the liver cell biomarkers CK18, ALB and AFP (**Figure 4D**, **4E**). We further assessed the ammonia concentration of the differentiated cells to see whether the induced cells possess liver cell functions. The outcomes demonstrated that after being exposed to MASM for 7 days, the ammonia concentration was reduced in the supernatant of cultures of EpCAM+ cells in a dose-dependent way (**Figure 4F**).

MASM suppresses the AKT/GSK3β/β-catenin pathway in EpCAM+ cells

In HCC cells, MASM inhibited the AKT/GSK3β/β-catenin pathway, as we had previously reported. To investigate if the inhibition of the AKT/

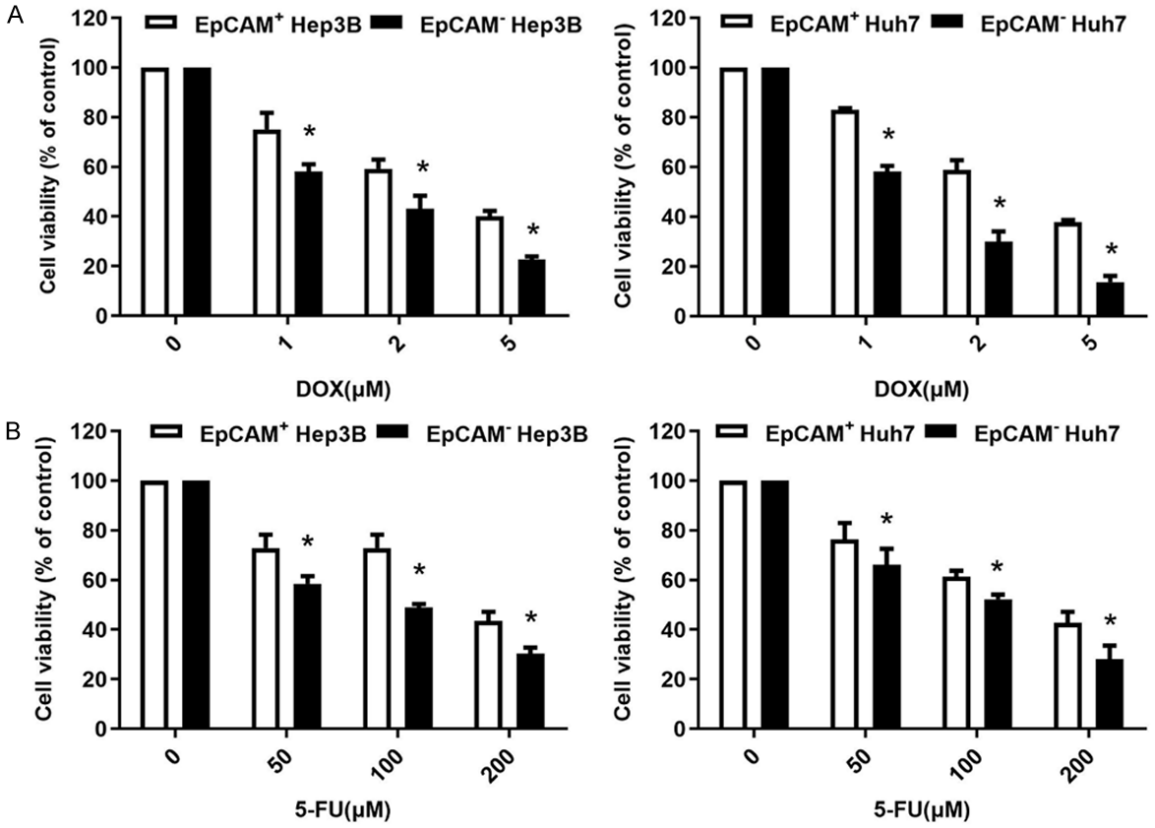

Figure 2. Chemoresistance of EpCAM+ cells. (A, B) Isolated EpCAM+ and EpCAM- cells were treated with 0, 1, 2, and 5 μM of DOX (A) or 0, 50, 100, and 200 μM of 5-FU (B) for 72 hours. Cell viability was determined by CCK-8 (white bar, EpCAM+ cells; black bar, EpCAM- cells). Data presented as mean ± SD were derived from 3 independent trials with triplicate wells per situation. *$P < 0.05$ vs. EpCAM+ cells.

GSK3β/β-catenin pathway contributed to the inhibitory actions of MASM on EpCAM+ cells, we treated EpCAM+ cells with series concentrations of MASM and specific AKT inhibitor MK-2206 (0.5 μM) or GSK3β inhibitor CHIR99021 (2.5 μM). The results showed that treatment with MK2206 resulted in slight inhibition of cell proliferation and spheroid formation, and co-treatment of EpCAM+ cells with MASM and MK2206 resulted in a greater inhibition than that observed with MASM alone (**Figure 5A**, **5B**). In contrast, CHIR99021 increased cell proliferation and spheroid formation, and antagonized effects of MASM on inhibiting the growth and spheroid formation of EpCAM+ cells.

Discussion

CSCs are one driving force of liver tumorigenesis and malignancy, and the therapies for HCC require the excision of CSCs [26]. Our earlier research has shown that MASM suppresses HCC cells, sphere cells and HCC xenograft growth via inhibiting the AKT/GSK3β/β-catenin signaling pathway [17]. However, the impact of MASM on CSCs is not yet understood.

In this study, we successfully isolated EpCAM+ cells from Hep3B and Huh7. EpCAM+ cells had significantly higher colony-formation ability and stronger proliferative capacity *in vitro* than EpCAM- cells. In addition, EpCAM+ cells were more resistant to cytotoxic chemotherapy such as DOX and 5-FU, in comparison with the EpCAM- population. These findings suggest that EpCAM+ cells possess CSC-like properties. Using these CSC-like cells, we found that MASM treatment significantly inhibited the proliferation of EpCAM+ cells, whereas it did not significantly induce the apoptosis of EpCAM+ cells as assessed by FACS. In addition, MASM caused an obvious reduction not only for primary spheroids, but also for spheroids in the subsequent two passages without MASM. RT-PCR analysis showed that treatment of MASM reduced the expressions of stemness genes CD133, EpCAM

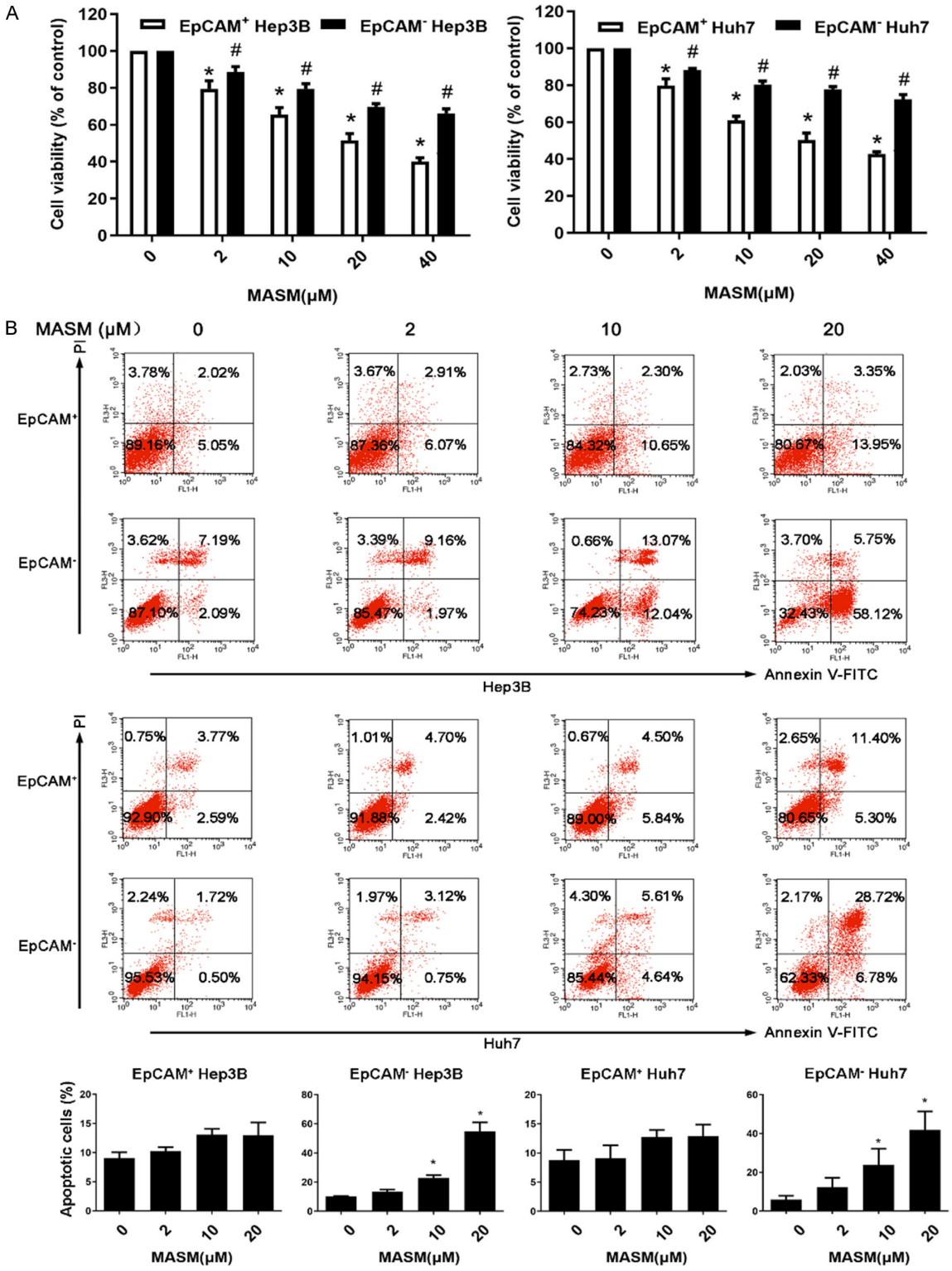

Figure 3. Effect of MASM on the proliferation and apoptosis of EpCAM+ and EpCAM- cells. A. EpCAM+ and EpCAM- cells were isolated from Hep3B and Huh7, and after being exposed to different doses of MASM (0, 2, 10, 20, and 40 μmol/L) for 72 hours, cell viability was determined by CCK-8. The results presented as the mean ± SD were from 3 independent experiments. *$P < 0.05$ vs. control cells, #$P < 0.05$ vs. EpCAM+ cells. B. Different doses of MASM (0, 2, 10, and 20 μmol/L) were added into the 6-well culture plates and incubated for 72 hours. Apoptotic cells were determined by flow cytometry. Graph of percentages of apoptotic cells are shown. $n = 3$. Mean ± SD. *$P < 0.05$ vs. control.

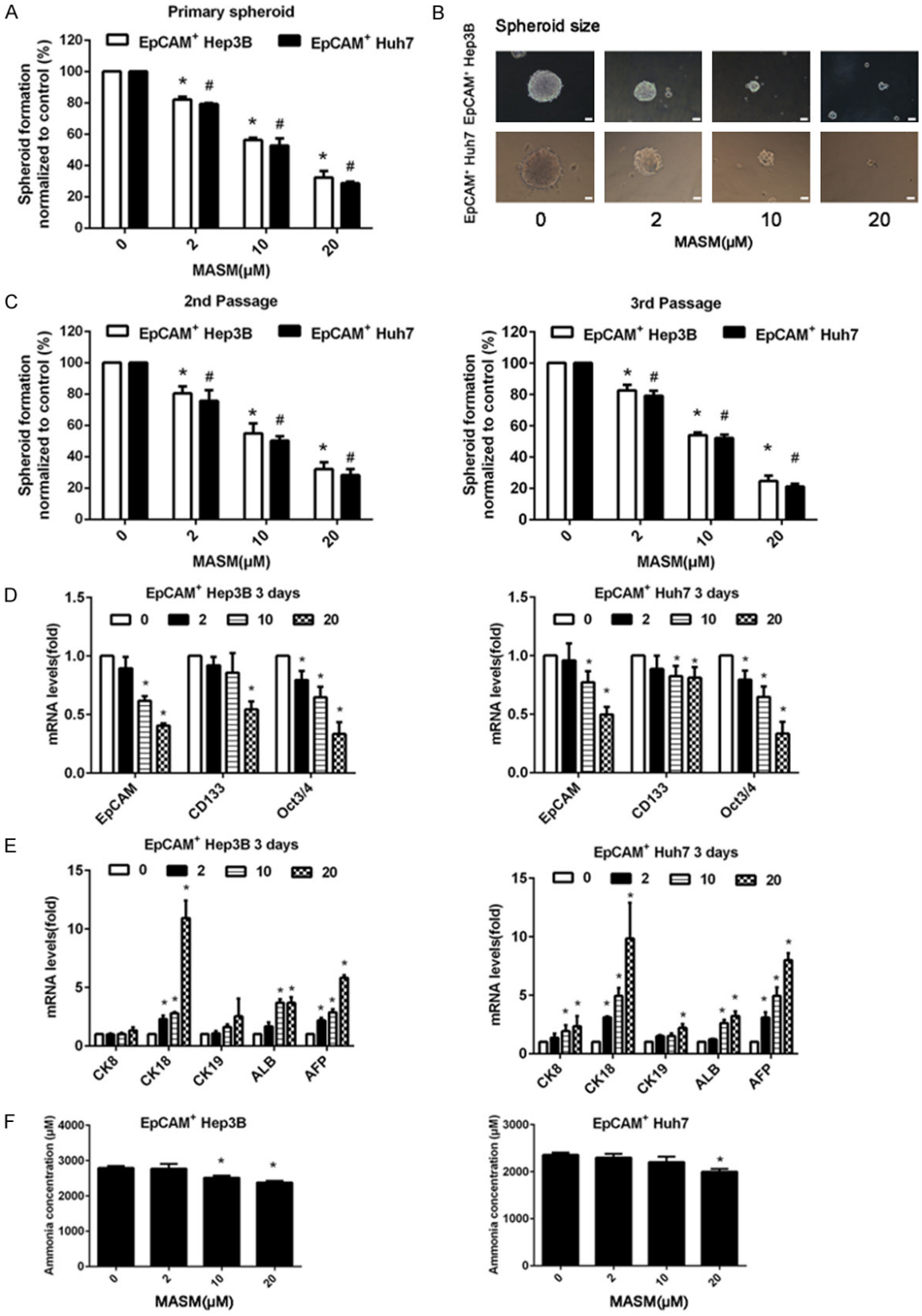

Figure 4. MASM inhibits CSC-like properties of EpCAM+ cells *in vitro*. A. MASM suppressed primary spheroid formation. *n* = 3. Mean ± SD. B. MASM decreased the dimensions of main spheroids (Scale bar = 100 μm). C. MASM-

treated spheroids exhibited reduced self-generation abilities. In the lack of MASM, MASM-treated primary spheroids created less spheroids in the subsequent two pathways compared with the control-treated primary spheroids. *n* = 3. Mean ± SD. **P* < 0.05 vs. untreated EpCAM+ Hep3B cells, #*P* < 0.05 vs. untreated EpCAM+ Huh7 cells. D, E. qRT-PCR analysis were used to determine the effect of MASM on the expressions of stem cell markers (EpCAM, CD133, and Oct3/4) and hepatocyte markers (CK18, ALB, and AFP). The mRNA levels were normalized to β-actin and relative to the control. *n* = 3. Mean ± SD. **P* < 0.05 *vs.* control. F. Ammonia concentration of EpCAM+ cells was decreased by MASM in a concentration-dependent manner. *n* = 3. Mean ± SD. **P* < 0.05 vs. control.

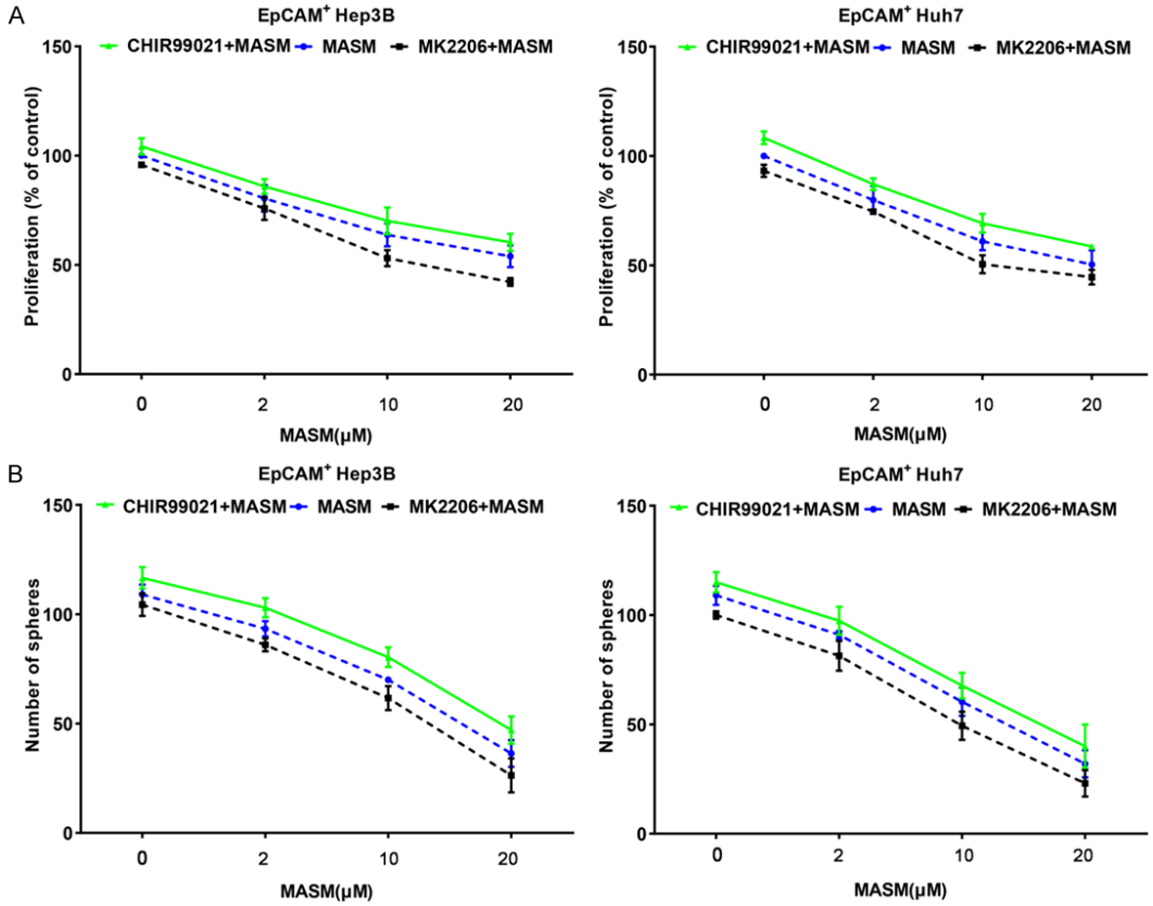

Figure 5. MASM suppresses the AKT/GSK3β/β-catenin pathway *in vitro.* A. Proliferation of EpCAM+ cells treated with MASM, MASM and MK2206 (0.5 μM), or MASM and CHIR99021 (2.5 μM). *n* = 3. B. Spheroid formation of EpCAM+ cells treated with MASM, MASM and MK2206 (0.5 μM), or MASM and CHIR99021 (2.5 μM). *n* = 3.

and Oct3/4, demonstrating that MASM affected the stemness of EpCAM+ cells. To further study the hepatocyte differentiation potential of isolated EpCAM+ cells, we evaluated the gene expression of hepatocytic and cholangiocytic biomarkers using RT-PCR. MASM elevated the expression of the liver-related genes (CK18, ALB, and AFP) in a dose-dependent manner. However, isolated EpCAM+ cells were expressing CK-19, an indicator for bile epithelial cells, at low levels after treatment of MASM, demonstrating that MASM induces CSC-like cells to differentiate into hepatocytes. Hepatocyte differentiation was further examined by functional tests using ammonia metabolism analysis, a typical test for the detection of hepatocyte function [27, 28]. Our data showed that the MASM-treated EpCAM+ cells not only expressed hepatocyte-specific biomarkers but also possessed the features of functional hepatocytes. In summary, the MASM-induced reduction of CSC-like properties was related to the inhibition of self-regeneration and the support of differentiation from CSC-like cells to functional hepatocytes.

Wnt/β-catenin signaling is one of the important pathways thought to be involved in CSCs self-

renewal [29]. A previous study showed that stimulation of Wnt-β-catenin signaling could induce EpCAM expression [30]. Our preliminary results showed that MASM inhibited hepatoma cell proliferation, led to cell death and growth arrest, inhibited sphere cells and suppressed the AKT/GSK3β/β-catenin signaling pathways [17]. Recently, our group has reported that WM130, another matrine analog, substantially suppressed CSC-like cells, and this impact may be through the reduction of the AKT/GSK3β/β-catenin pathway [31]. Thus, we speculated that the inhibition of MASM on CSC-like cells may be correlated with the suppression of the AKT/GSK3β/β-catenin pathway. Data presented in this study showed that MK2206 suppressed, whereas CHIR99021 elevated EpCAM+ cell proliferation and spheroid production. Notably, co-treatment of EpCAM+ cells with MASM and MK2206 had an additive impact, while CHIR-99021 antagonized MASM's impact. These findings revealed that the suppression impact of MASM on CSC-like cells was modulated by suppressing the AKT/GSK3β/β-catenin signaling pathway.

Conclusions

In conclusion, our data revealed that MASM suppressed the self-renewal of EpCAM+ cells and promoted the differentiation from CSC-like cells to hepatocytes. These effects were accompanied with the down-regulation of the AKT/GSK3β/β-catenin pathway. The findings may shed light on the potential clinical utility of MASM in treating HCC.

Acknowledgements

The study was funded by the Shanghai Nature Science Foundation (grant No. 19ZR1419600) and the project of Shanghai University Young Talents Launch (grant.N.13-G210-22-432).

Disclosure of conflict of interest

None.

Address correspondence to: Drs. Ying Liu and Shipeng He, Institute of Translational Medicine, Shanghai University, No. 99 Shangda Road, Shanghai 200444, China. E-mail: liuchanger1984@163.com (YL); heshipeng@shu.edu.cn (SPH)

References

[1] Piñero F, Dirchwolf M and Pessôa MG. Biomarkers in hepatocellular carcinoma: diagnosis, prognosis and treatment response assessment. Cells 2020; 9: 1370.

[2] Yang JD, Hainaut P, Gores GJ, Amadou A, Plymoth A and Roberts LR. A global view of hepatocellular carcinoma: trends, risk, prevention and management. Nat Rev Gastroenterol Hepatol 2019; 16: 589-604.

[3] Forner A, Reig M and Bruix J. Hepatocellular carcinoma. Lancet 2018; 391: 1301-1314.

[4] Sahu SK, Chawla YK, Dhiman RK, Singh V, Duseja A, Taneja S, Kalra N and Gorsi U. Rupture of hepatocellular carcinoma: a review of literature. J Clin Exp Hepatol 2019; 9: 245-256.

[5] Hartke J, Johnson M and Ghabril M. The diagnosis and treatment of hepatocellular carcinoma. Semin Diagn Pathol 2017; 34: 153-159.

[6] Liu YC, Yeh CT and Lin KH. Cancer stem cell functions in hepatocellular carcinoma and comprehensive therapeutic strategies. Cells 2020; 9: 1331.

[7] Brown HK, Tellez-Gabriel M and Heymann D. Cancer stem cells in osteosarcoma. Cancer Lett 2017; 386: 189-195.

[8] Butti R, Gunasekaran VP, Kumar TVS, Banerjee P and Kundu GC. Breast cancer stem cells: biology and therapeutic implications. Int J Biochem Cell Biol 2019; 107: 38-52.

[9] Atashzar MR, Baharlou R, Karami J, Abdollahi H, Rezaei R, Pourramezan F and Zoljalali Moghaddam SH. Cancer stem cells: a review from origin to therapeutic implications. J Cell Physiol 2020; 235: 790-803.

[10] Haraguchi N, Utsunomiya T, Inoue H, Tanaka F, Mimori K, Barnard GF and Mori M. Characterization of a side population of cancer cells from human gastrointestinal system. Stem Cells 2006; 24: 506-513.

[11] Hu C, Li H, Li J, Zhu Z, Yin S, Hao X, Yao M, Zheng S and Gu J. Analysis of ABCG2 expression and side population identifies intrinsic drug efflux in the HCC cell line MHCC-97L and its modulation by Akt signaling. Carcinogenesis 2008; 29: 2289-2297.

[12] Pandit H, Li Y, Zheng Q, Guo W, Yu Y, Li S and Martin RCG. Carcinogenetic initiation contributed by EpCAM+ cancer cells in orthotopic HCC models of immunocompetent and athymic mice. Oncotarget 2020; 11: 2047-2060.

[13] Zhou L and Zhu Y. The EpCAM overexpression is associated with clinicopathological significance and prognosis in hepatocellular carcinoma patients: a systematic review and meta-analysis. Int J Surg 2018; 56: 274-280.

[14] Ji J, Yamashita T, Budhu A, Forgues M, Jia HL, Li C, Deng C, Wauthier E, Reid LM, Ye QH, Qin LX, Yang W, Wang HY, Tang ZY, Croce CM and Wang XW. Identification of microRNA-181 by genome-wide screening as a critical player in EpCAM-positive hepatic cancer stem cells. Hepatology 2009; 50: 472-480.

[15] Ogawa K, Tanaka S, Matsumura S, Murakata A, Ban D, Ochiai T, Irie T, Kudo A, Nakamura N, Tanabe M and Arii S. EpCAM-targeted therapy for human hepatocellular carcinoma. Ann Surg Oncol 2014; 21: 1314-1322.
[16] Park DJ, Sung PS, Kim JH, Lee GW, Jang JW, Jung ES, Bae SH, Choi JY and Yoon SK. EpCAM-high liver cancer stem cells resist natural killer cell-mediated cytotoxicity by upregulating CEACAM1. J Immunother Cancer 2020; 8: e000301.
[17] Liu Y, Qi Y, Bai ZH, Ni CX, Ren QH, Xu WH, Xu J, Hu HG, Qiu L, Li JZ, He ZG and Zhang JP. A novel matrine derivate inhibits differentiated human hepatoma cells and hepatic cancer stem-like cells by suppressing PI3K/AKT signaling pathways. Acta Pharmacol Sin 2017; 38: 120-132.
[18] Li X, Tang Z, Wen L, Jiang C and Feng Q. Matrine: a review of its pharmacology, pharmacokinetics, toxicity, clinical application and preparation researches. J Ethnopharmacol 2021; 269: 113682.
[19] Sun N, Zhang H, Sun P, Khan A, Guo J, Zheng X, Sun Y, Fan K, Yin W and Li H. Matrine exhibits antiviral activity in a PRRSV/PCV2 co-infected mouse model. Phytomedicine 2020; 77: 153289.
[20] Chen MH, Gu YY, Zhang AL, Sze DM, Mo SL and May BH. Biological effects and mechanisms of matrine and other constituents of Sophora flavescens in colorectal cancer. Pharmacol Res 2021; 171: 105778.
[21] Sun XY, Jia LY, Rong Z, Zhou X, Cao LQ, Li AH, Guo M, Jin J, Wang YD, Huang L, Li YH, He ZJ, Li L, Ma RK, Lv YF, Shao KK, Zhang J and Cao HL. Research advances on matrine. Front Chem 2022; 10: 867318.
[22] Lin Y, He F, Wu L, Xu Y and Du Q. Matrine exerts pharmacological effects through multiple signaling pathways: a comprehensive review. Drug Des Devel Ther 2022; 16: 533-569.
[23] Zhang L, Liu W, Zhang R, Wang Z, Shen Z, Chen X and Bi K. Pharmacokinetic study of matrine, oxymatrine and oxysophocarpine in rat plasma after oral administration of Sophora flavescens Ait. extract by liquid chromatography tandem mass spectrometry. J Pharm Biomed Anal 2008; 47: 892-898.
[24] Hu H, Wang S, Zhang C, Wang L, Ding L, Zhang J and Wu Q. Synthesis and in vitro inhibitory activity of matrine derivatives towards pro-inflammatory cytokines. Bioorg Med Chem Lett 2010; 20: 7537-7539.
[25] Hasan S, Taha R and Omri HE. Current opinions on chemoresistance: an overview. Bioinformation 2018; 14: 80-85.
[26] Lee TK, Guan XY and Ma S. Cancer stem cells in hepatocellular carcinoma - from origin to clinical implications. Nat Rev Gastroenterol Hepatol 2022; 19: 26-44.
[27] Yin C, Lin Y, Zhang X, Chen YX, Zeng X, Yue HY, Hou JL, Deng X, Zhang JP, Han ZG and Xie WF. Differentiation therapy of hepatocellular carcinoma in mice with recombinant adenovirus carrying hepatocyte nuclear factor-4alpha gene. Hepatology 2008; 48: 1528-1539.
[28] Jung KH, Zhang J, Zhou C, Shen H, Gagea M, Rodriguez-Aguayo C, Lopez-Berestein G, Sood AK and Beretta L. Differentiation therapy for hepatocellular carcinoma: multifaceted effects of miR-148a on tumor growth and phenotype and liver fibrosis. Hepatology 2016; 63: 864-879.
[29] Jiménez-Guerrero R, Belmonte-Fernández A, Flores ML, González-Moreno M, Pérez-Valderrama B, Romero F, Japón MÁ and Sáez C. Wnt/β-catenin signaling contributes to paclitaxel resistance in bladder cancer cells with cancer stem cell-like properties. Int J Mol Sci 2021; 23: 450.
[30] Yamashita T, Budhu A, Forgues M and Wang XW. Activation of hepatic stem cell marker EpCAM by Wnt-beta-catenin signaling in hepatocellular carcinoma. Cancer Res 2007; 67: 10831-10839.
[31] Ni CX, Qi Y, Zhang J, Liu Y, Xu WH, Xu J, Hu HG, Wu QY, Wang Y and Zhang JP. WM130 preferentially inhibits hepatic cancer stem-like cells by suppressing AKT/GSK3β/β-catenin signaling pathway. Oncotarget 2016; 7: 79544-79556.